Intelligent and Application-Oriented Optimal Design of Travelling Field Flux Pumps

Giacomo Russo, Mohammad Yazdani-Asrami, *Senior Member, IEEE*, Massimo Fabbri, and Antonio Morandi, *Senior Member, IEEE*

***Abstract*—Flux pumping based on traveling field is a promising technology, potentially able to produce breakthrough innovation in the supply of HTS magnets, which offers a contactless, low-voltage, and high-current alternative to power electronics exciters and current leads solutions. However, their engineering process has proved to present major challenges. Previous studies have empirically investigated, either numerically or experimentally, the impact of individual design parameters on the outputs and performance of flux pumps, but they were only able to provide qualitative relations that are not suitable for proper designing actions. In this study, we propose a new approach based on artificial intelligence (AI) techniques to generate effective flux pump designs. A finite element (FE) model, previously validated against experimental results, was employed in this procedure to provide a relation between the design parameters of the flux pump and the objective function of the optimization problem, that is the maximum efficiency during persistent operation. The FE model is exploited in the form of a function that is fed into AI-based optimization algorithms such as the genetic algorithm and the particle swarm optimization. The established procedure offers a "systematic" method for the design of viable and efficient flux pumps for contactless energization HTS magnets in real applications.**

***Index Terms*—DC superconducting magnet, design optimization, flux pump, fusion magnet, HTS dynamo, HTS power supply.**

I. Introduction

SUPERCONDUCTING magnets are widely recognized to be the only viable solution for applications like nuclear fusion [1] and particle accelerators [2]. Recent breakthroughs in the development of High Temperature Superconducting (HTS) magnets [3] are making a stronger case for their industrial commercialization in fusion [4], [5], [6] and opening also new market opportunities like aerospace [7], [8], [9], [10], [11]. However, the energization of HTS magnets poses real challenges and obstacles towards their practical application. Metal current leads, that physically connect the terminals of the magnet at cryogenic temperatures to a controlled current source operating at room temperature, significantly contribute to the total cryogenic heat load in the magnet systems due to persistent heat conduction and joule loss [12]. This impact extends to both capital and operational costs [13]. Additionally, providing a room temperature solid-state power supply capable of energizing and sustaining a high current inductive load can be largely energy intensive and involve a considerable amount of reactive power [14].

For many decades, flux pumps have been considered a promising solution to the aforementioned problems because of their compactness and since they provide contactless energization of superconducting magnets allowing for extremely low-loss quasi-persistent current mode after the first ramp-up [15], [16], [17], [18], [19]. Despite long-lasting research on these devices, their complex and counterintuitive physical mechanism has prevented their engineering development and, therefore, validation in a relevant environment to fulfill the requirements of real applications. However, recent progresses in numerical modelling have contributed to reduce this research gap [20], [21], [22], [23]. In addition, several studies have focused on the impact of the design parameters on the performance, including: the frequency of rotation [24], the ratio between the permanent magnet and HTS tape widths [25], the air gap [26], the number of permanent magnets [27] and their geometry [28]. Nevertheless, to date, no analytical sets of formulas (so-called analytical design routine) have been derived to address the design of flux pumps because of the many intricacies related to the non-monotone and highly nonlinear interdependencies between the design parameters [29].

In this study, we have addressed the research gap related to the lack of flux pumps design tools by proposing an optimization method based on artificial intelligence (AI) techniques [30], [31]: the genetic algorithm (GA) [32] and the particle swarm optimizer (PSO) [33]. For the flux pump topology to apply this method to, we have chosen the HTS dynamo [34], [35], because of the larger availability of numerical tools and experimental results that allowed us to make the initial necessary design assumptions. However, this method is conceived to yield a replicable designing routine that is widely applicable to other layouts as well, like the linear type flux pump [36], [37]. In this study we have developed this designing procedure addressing one real case study: the Toroidal Field (TF) module coil of the Divertor Tokamak Test (DTT) facility, currently under construction in ENEA-Frascati, Italy [38], [39].

The paper is structured as follows: Section II describes the design procedure including the optimization problem formulation

Received 23 September 2024; revised 18 November 2024; accepted 19 November 2024. Date of publication 11 December 2024; date of current version 31 December 2024. *(Corresponding author: Giacomo Russo.)*

Giacomo Russo, Massimo Fabbri, and Antonio Morandi are with the Department of Electrical, Electronic and Information Engineering, University of Bologna, 40136 Bologna, Italy (e-mail: giacomo.russo5@unibo.it).

Mohammad Yazdani-Asrami is with the CryoElectric Research Lab, Propulsion, Electrification, and Superconductivity Group, Autonomous Systems and Connectivity Division, James Watt School of Engineering, University of Glasgow, G12 8QQ Glasgow, U.K. (e-mail: m.yazdaniasrami@gmail.com).

Color versions of one or more figures in this article are available at https://doi.org/10.1109/TASC.2024.3509405.

Digital Object Identifier 10.1109/TASC.2024.3509405

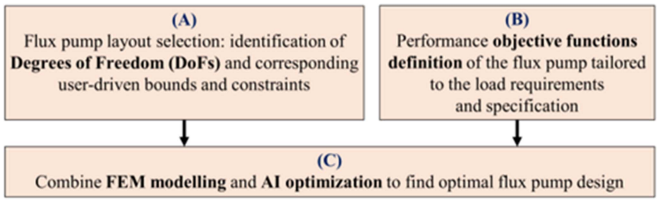

Fig. 1. Application-oriented designing procedure of flux pumps flowchart scheme.

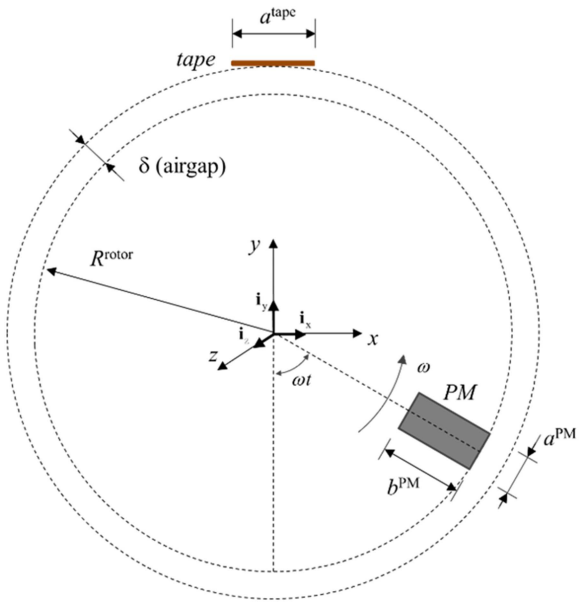

Fig. 2. 2D schematic of the HTS dynamo reporting its main geometrical parameters (figure previously published in SUST by the present authors [20]).

and the assumptions of the considered case study, Section III reports the optimization results and discusses the characteristics of the optimized flux pump, and finally Section IV summarizes the conclusions.

II. Designing Procedure

The flowchart of the replicable design procedure developed in this study is shown in Fig. 1.

A. Phase (A)

In this study, the design parameters of flux pump to be found for ensuring optimal performance are referred to as the Degrees of Freedom (Dofs) of the optimization problem. The Dofs are flux pump topology specific, therefore the first step is choosing the flux pump layout. As explained earlier, among all types of flux pumps [18] the HTS dynamo has been chosen for this specific study. Fig. 2 depicts a 2D schematic of a dynamo with only one HTS tape and one permanent magnet to highlight its main geometrical specifications [20]. In principle, all design parameters could be set as Dofs in the optimization algorithm to find their best combination according to the objective function and constraints. However, we identify a subset of dynamo specifications to which we assign a constant value and call these

TABLE I
Assigned Parameters and Dofs Bounds of the HTS Dynamo for Supplying the DTT TF Coil Module

	Specification	Value or bounds
Assigned parameters	Width of the permanent magnets (PMs), a^{PM}	3.2 mm
	Height of the PMs, b^{PM}	12.7 mm
	Remanence of the PMs, B_r	1.3 T
	Airgap between the PM and the HTS tape, δ	1 mm
	Axial length	1 m
	Operating temperature	77 K
	HTS tape model and manufacturer	SuperOx YBCO 2G HTS
Optimization degrees of freedom (Dofs)	Number of PMs	1 - 250
	Width of the HTS tape, a^{tape}	6 mm – 24 mm
	External radius of the rotor, R^{rotor}	1 m – 2 m
	Frequency of rotation of the PMs, f	1 Hz – 25 Hz

assigned parameters. We do this to minimize the number of times the optimizer has to run the objective function consisting of a relatively computationally expensive finite element (FE) method [20]. Since previous studies have shown that the impact of some specifications is predictable and monotone, the approach to assign their values is not only computationally efficient but also practical. The dynamo specifications left free to vary are therefore the Dofs, for which lower and upper bounds are chosen.

Table I lists the assigned parameters and the Dofs and their values and bounds, respectively. The choices of using the SuperOx YBCO 2G HTS tape at 77 K are made for optimal efficiency performance based on previous findings in [22]. The airgap is set to the lowest reasonable value of 1 mm because of its known impact on performance [26] and the commercially available permanent magnets (PMs) are the same as already employed in [34] and [22]. Since performance is driven by the PM-to-tape width ratio [28], varying the tape width alone is sufficient. For greater flexibility, however, users may choose to treat both widths as optimizable parameters according to specific design needs. As per the Dofs bounds, the large maximum rotor radius of 2 m is justified by the much larger conventional power supply and current leads infrastructure that is being installed at the DTT ENEA-Frascati premises [38]. The maximum number of mountable PMs on the rotor is determined by the number that allows them to be spaced apart by a measure equal to the maximum width of the HTS tape. The tape width bounds are chosen based on typical commercially available dimensions, which are 6 and 24 mm. Finally, frequencies of rotation in the range of 1 Hz to 25 Hz are chosen because it's known from literature that higher values result in rapid increase of losses [24].

B. Phase (B)

The optimization objective and constraints are defined by the rated current of the HTS magnet (I_{rated}.), set at 42.5 kA for

the DTT TF coil module, and a maximum acceptable current ramp-up time, assumed to be 2000 s [39]. Assuming a linear electrical characteristic of the flux pump and an operating condition of maximum efficiency around half of its current capability, as previously reported in [20], the optimization constraint is set such that the flux pump must be able to inject up to twice the I_{rated}. Another flux pump constraint is the minimum output voltage that depends on the maximum acceptable charging time. Considering that the inductance of the DTT TF coil module is 48 mH [39], the flux pump output voltage at rated current (hereafter referred to as V_{rated}) should be no lower than a threshold value that we refer to as V_{target}, which for our case study is equal to 1 V to produce a ramp rate not lower than 20 A/s on the load coil with 48 mH inductance so to reach the current I_{rated} in no more than 2000 s.

C. Phase (C)

The 2D FE equivalent circuit-based numerical model - previously explained in [20] and validated against experimental results in [22] - is implemented in the form of a function in MATLAB to calculate the dynamo performance (efficiency, open circuit output voltage, limit current in generator mode [19]) based on a specific combination of Dofs. The FE model solves (1) and (2).

$$\bar{\bar{M}}\frac{d\bar{I}_w}{dt} = -\bar{\bar{R}}\,\bar{I}_w - \bar{u} - \bar{1}V \tag{1}$$

$$\bar{1}^T\bar{I}_w = I_{tot} \tag{2}$$

where V is the resulting voltage at the terminals of the flux pump, $\bar{I}_w$ is the set of currents of the tape mesh elements, $\bar{1}$ is a column vector of as many ones as the number of mesh elements, $M^=$ is the self/mutual induction coefficients matrix, $R^=$ is the diagonal matrix of resistances, I_{tot} is the transport current of the flux pump tape, and $\bar{u}$ is the forcing term that is obtained based on the derivative of the external magnetic vector potential produced by the PMs. Using the same approach as in [20] for obtaining the electrical characteristic of the dynamo, for each combination of Dofs, (1) and (2) are solved for $I_{tot} = 0$ A, 600 A, and 1200 A to find the generator mode current limit (hereafter referred to as I_{lim}, i.e., the value of I_{tot} at which $V = 0$) by interpolation. The choice of scanning the electrical characteristic for $I_{tot} =$ 0 A, 600 A, and 1200 A has been taken after several attempts to make sure that I_{lim} was being accurately found for every possible Dofs combination. Next, the maximum efficiency is calculated assuming operation at $I_{tot} = I_{lim}/2$ [20], while V_{oc} corresponds to the computed value of V of (1) for $I_{tot} = 0$ A. It must be specified that each function calculation is carried out assuming only one HTS tape on the rotor. This is necessary because several dozens of tapes in parallel are needed to reach I_{rated}, and simulating all of them would require extremely long computation time for one run, incompatible with optimization algorithms. This issue is overcome by multiplying the value of I_{lim} obtained with a single tape by the number of tapes that can be connected electrically in parallel. The latter is found considering that each tape is azimuthally equally spaced, and they cannot occupy more than one third of the total circumference at their disposal (this is imposed to assure they do not significantly magnetically affect each other). In support to this step, there are numerous previous experimental studies that show that I_{lim} varies proportionally with the number of tapes or flux pumps modules electrically in parallel [42], [43].

For the case study of the DTT TF coil module, the dynamo performance constraints are:

$$V_{rated} > V_{target} \tag{3}$$

$$I_{lim} = 2{*}I_{rated} \tag{4}$$

(3) serves to respect the coil maximum ramp-up time and (4) is the equality constraints that assures that for $I_{tot} = I_{rated}$ the dynamo operate close to its maximum efficiency point, similar to the approach employed in [21]. (3) and (4) plus the objective of maximizing the efficiency at $I_{tot} = I_{lim}/2$, that we refer to as η_{rated}, are incorporated in a single objective function, that is fed to the GA and PSO, implementing the fuzzy logic [44], [45]. To represent these objectives and constraints in a fuzzy logic framework, individual membership functions are defined. The efficiency of the flux pump, defined in [20] as the ratio between the integral over a rotation period of the power V×I delivered to the load, and the integral over the same period of the input mechanical power, calculated as the sum of the delivered power and internal losses, is represented by a membership function (F_{eff}) that linearly varies from 0 to 1 for the efficiency ranging from 0% to its maximum attainable value. After carrying out unconstrained optimization simulations, the latter is found equal to 30%. To account (3) and (4) as constraints, their membership functions (F_V and F_I) also range from 0 to 1, but they abruptly decay for V_{rated} and I_{lim} being below V_{target} and $2 * I_{rated}$ respectively rather than varying proportionally. This is done implementing (5) and (6).

$$F_V = \begin{cases} 1 \text{ if } V_{rated} \geq V_{target} \\ \left(\frac{V_{oc}}{V_{target}}\right)^5 \text{ if } V_{rated} < V_{target} \end{cases}. \tag{5}$$

$$F_I = \begin{cases} 1 \text{ if } I_{lim} \geq 2 * I_{rated} \\ \left(\frac{I_{lim}}{2*I_{rated}}\right)^5 \text{ if } I_{lim} < 2 * I_{rated} \end{cases}. \tag{6}$$

Therefore, the objective function to be maximized is represented in (7).

$$Objective\ function = \min\left(F_{eff}, F_V, F_I\right) \tag{7}$$

Finally, we mention that we have used 10 and 100 for the PSO's swarm size and number of iterations, respectively, as well as for the GA's size of population and number of generations.

III. Results and Discussion

The optimization results using the GA and PSO are reported in Table II .

It can be observed that both the GA and the PSO managed to find a Dofs combination that maximizes the dynamo efficiency while satisfying the current and voltage constraints. It is also interesting to note that the two optimizers converge toward two very similar Dofs combinations, where the width of each HTS tape and the external radius of the rotor are very close, if not equal to, their corresponding upper bounds. The overall best solution in terms of efficiency is the one emerging from the

TABLE II
RELEVANT SPECIFICATIONS OF THE DTT TF COIL MODULE

Specification	Value
Rated current [39]	42.5 kA
Inductance [39]	48 mH
Ramp-up duration [39]	2000 s
Series joint resistance [40], [41]	100 nΩ

TABLE III
SPECIFICATION OF THE OPTIMIZED HTS DYNAMOS AND THE CORRESPONDING MOST RELEVANT PERFORMANCE

		Optimization results	
	Specifications	**GA**	**PSO**
Dofs results	Width of the HTS tape, a^{tape}	23.8 mm	23.5 mm
	Number of HTS tapes in parallel	94	90
	Number of PMs	124	121
	Frequency of rotation of the PMs, f	12.7 Hz	12.1 Hz
	External radius of the rotor, R^{rotor}	1.73 m	2 m
Performance	η_{rated}	18.9%	19.1%
	I_{lim}	85.4 kA	85.6 kA
	V_{rated}	1.17 V	1.13 V

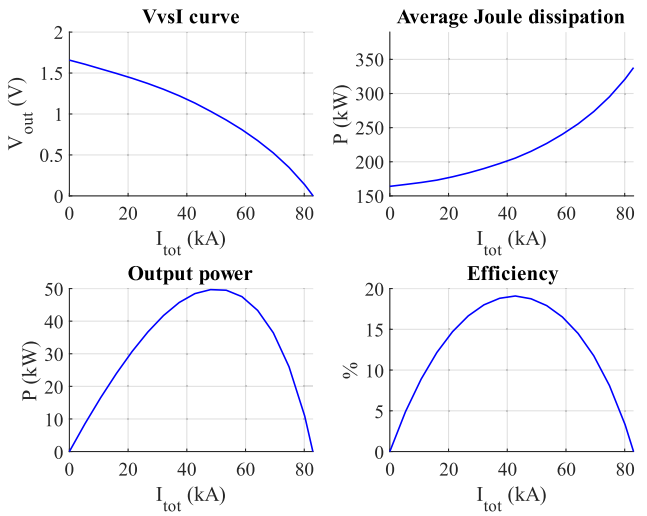

Fig. 3. Characterization of the optimized HTS dynamo obtained with the PSO optimizer.

PSO (19.1% when $I_{lim} = 2 * I_{rated}$) while a more compact design (1.73 m rotor radius) is found with the GA. Fig. 3 shows the performance characteristics of the HTS dynamo obtained with the PSO. Plots shown were obtained from detailed FE analysis performed afterward for the designed flux pump in all the range of current from 0 to I_{lim}. It can be observed from the quasi-linear electrical characteristic (V vs I curve) and the Efficiency plot, whose maximum is around $I_{tot} = I_{lim}/2$, that the approximations applied based on the previous observation of [20] are confirmed to be valid. At $I_{tot} = 42.5$ kA, the HTS

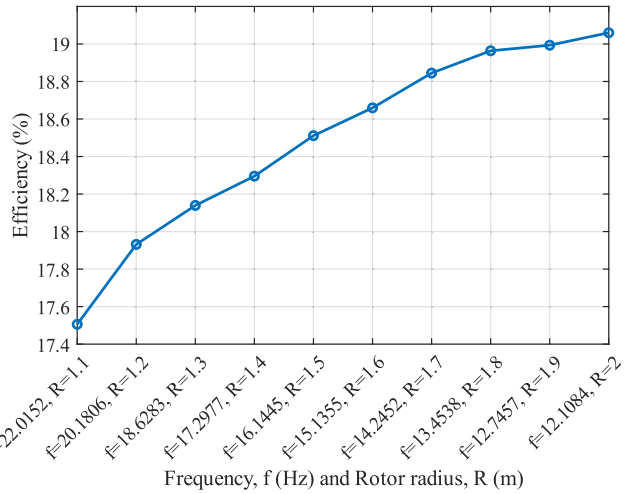

Fig. 4. Sensitivity analysis of η_{rated} depending on the rotor radius while maintaining a constant tip speed by increasing the rotation frequency.

dynamo dissipates slightly more than 200 kW at 77 K while delivering about 47.5 kW. Despite the aforementioned power loss sounds enormous, as it happens at cryogenic temperature, it is reminded that at steady state (after the first ramp up of the magnet current is completed) the flux pump can be operated using a hysteresis control that remains in lossless quasi-persistent current mode for the large majority of the time, thus reducing the average power consumption during this operating condition to 1.05 kW, which is calculated using (8) of [37].

The major difference between the GA and PSO results is related to the values of the external radius of the rotor, that is 1.73 m and 2 m for the GA and the PSO, respectively. It is also noted that for such a difference in rotor radius, the improvement in η_{rated} looks marginal (only 0.2%). To explore the possibility of making the HTS dynamo more compact without compromising efficiency, a sensitivity analysis is conducted to evaluate how performance changes when the rotor radius decreases while maintaining a constant tip speed by increasing the rotation frequency. The results of the sensitivity analysis are shown in Fig. 4, where it can be seen that an almost 50% R^{rotor} reduction (from 2 m to 1.1 m) results in only a 1.6% efficiency decrease (from 19.1% to about 17.5%).

IV. CONCLUSION

In this study, we developed an application-oriented design procedure for travelling field flux pumps (HTS dynamos and linear type). Starting from the operating conditions (e.g., rated current) and requirements (e.g., acceptable ramp-up time) of the superconducting magnet to be energized, we identified the flux pump design parameters and defined its objectives and constraints. Next, we formulated a single objective function incorporating these using the fuzzy logic. Artificial Intelligence algorithms, such as genetic algorithm (GA) and particle swarm optimizer (PSO), were then employed to solve the optimization problem. Applying this procedure to a coil module of the Toroidal field of the DTT, we found that GA and PSO converged on similar results that met all constraints.

REFERENCES

[1] N. Mitchell and A. Devred, "The ITER magnet system: Configuration and construction status," *Fusion Eng. Des.*, vol. 123, pp. 17–25, 2017.

[2] P. Védrine et al., *Chapter 2: High-Field Magnets*. Meyrin, Switzerland: CERN, Mar. 2022. [Online]. Available: https://e-publishing.cern.ch/index.php/CYRM/article/view/1345

[3] A. Godeke, "High temperature superconductors for commercial magnets," *Supercond. Sci. Technol.*, vol. 36, no. 11, 2023, Art. no. 113001.

[4] Z. S. Hartwig et al., "The SPARC toroidal field model coil program," *IEEE Trans. Appl. Supercond.*, vol. 34, no. 2, Mar. 2024, Art. no. 0600316.

[5] R. F. Vieira et al., "Design, fabrication, and assembly of the SPARC toroidal field model coil," *IEEE Trans. Appl. Supercond.*, vol. 34, no. 2, Mar. 2024, Art. no. 0600615.

[6] D. Whyte et al., "Experimental assessment and model validation of the SPARC toroidal field model coil," *IEEE Trans. Appl. Supercond.*, vol. 34, no. 2, Mar. 2023, Art. no. 0600218.

[7] L. Ybanez et al., "ASCEND: The first step towards cryogenic electric propulsion," in *Proc. IOP Conf. Ser.: Mater. Sci. Eng.*, IOP Publishing, 2022, Art. no. 012034.

[8] M. A. La Rosa Betancourt, E. Bögel, M. R. Collier-Wright, P. Kaplan, and J. Wilcox, "High-temperature superconductors as a key enabling technology for space missions," *Adv. System Computations Eng. Des.*, vol. 2021, 2021, Art. no. 4110.

[9] M. Collier-Wright et al., "High-temperature superconductor-based power and propulsion system architectures as enablers for high power missions," *Acta Astronaut*, vol. 201, pp. 198–208, 2022.

[10] J. R. Olatunji, M. Goddard-Winchester, B. Mallett, N. Strickland, and R. Pollock, "Design of a superconducting magnet for space propulsion on the international space station," *IEEE Trans. Appl. Supercond.*, vol. 34, no. 3, May 2024, Art. no. 3601006.

[11] M. Yazdani-Asrami, M. Zhang, and W. Yuan, "Challenges for developing high temperature superconducting ring magnets for rotating electric machine applications in future electric aircrafts," *J. Magn. Magn. Mater.*, vol. 522, 2021, Art. no. 167543.

[12] A. Ballarino, "Current leads, links and buses," 2015, doi: 10.5170/CERN-2014-005.547. [Online]. Available: https://cds.cern.ch/record/1974072

[13] S. S. Kalsi, *Applications of High Temperature Superconductors to Electric Power Equipment*. Hoboken, NJ, USA: John Wiley & Sons, 2011.

[14] D. Jia, J. Tao, R. Fan, and J. Lu, "Research on coordinated control strategy of ITER power supplies and reactive power compensation system," *J. Fusion Energy*, vol. 39, pp. 491–499, 2020.

[15] N. Felici, "De l'équilibre et dumouvement des supraconducteurs," *Annales de Physique*, vol. 31, no. 13, pp. 266–349, 1940.

[16] J. Van Suchtelen, J. Volger, and D. Van Houwelingen, "The principle and performance of a superconducting dynamo," *Cryogenics*, vol. 5, no. 5, pp. 256–266, 1965.

[17] H. ten Kate and L. van de Klundert, "Fully superconducting rectifiers and flux Pumps," *Cryogenics*, vol. 21, pp. 195–267, 1981.

[18] T. Coombs, "Superconducting flux pumps," *J. Appl. Phys.*, vol. 125, 2019, Art. no. 23.

[19] Z. Wen, H. Zhang, and M. Mueller, "High temperature superconducting flux pumps for contactless energization," *Crystals*, vol. 12, no. 6, 2022, Art. no. 766.

[20] A. Morandi, G. Russo, M. Fabbri, and L. Soldati, "Energy balance, efficiency and operational limits of the dynamo type flux pump," *Supercond. Sci. Technol.*, vol. 35, no. 6, 2022, Art. no. 065011.

[21] G. Russo and A. Morandi, "A numerical study on the energization of the field coils of a full-size wind turbine with different types of flux pumps," *Energies*, vol. 15, no. 15, 2022, Art. no. 5392.

[22] G. Russo and A. Morandi, "Evaluation of the performance of commercial high temperature superconducting tapes for dynamo flux pump applications," *Energies*, vol. 16, no. 21, 2023, Art. no. 7244.

[23] M. D. Ainslie, "Numerical modelling of high-temperature superconducting dynamos: A review," *Superconductivity*, vol. 5, 2023, Art. no. 100033.

[24] C. W. Bumby et al., "Frequency dependent behavior of a dynamo-type HTS flux pump," *IEEE Trans. Appl. Supercond.*, vol. 27, no. 4, Jun. 2016, Art. no. 5200705.

[25] A. E. Pantoja, Z. Jiang, R. A. Badcock, and C. W. Bumby, "Impact of stator wire width on output of a dynamo-type HTS flux pump," *IEEE Trans. Appl. Supercond.*, vol. 26, no. 8, Dec. 2016, Art. no. 4805208.

[26] Z. Jiang, C. W. Bumby, R. A. Badcock, H.-J. Sung, N. J. Long, and N. Amemiya, "Impact of flux gap upon dynamic resistance of a rotating HTS flux pump," *Supercond. Sci. Technol.*, vol. 28, no. 11, 2015, Art. no. 115008.

[27] P. Zhou et al., "Impact of magnet number on the DC output of a dynamo-type HTS flux pump," *IEEE Trans. Appl. Supercond.*, vol. 33, no. 8, Nov. 2023, Art. no. 4603509.

[28] R. A. Badcock et al., "Impact of magnet geometry on output of a dynamo-type HTS flux pump," *IEEE Trans. Appl. Supercond.*, vol. 27, no. 4, Jun. 2017, Art. no. 5200905.

[29] E. Guerra, *Dimensionamento Di Un Impiando Di Alimentazione Contactless Di Tipo Dynamo Flux Pump Per Magneti Superconduttivi Di Centrali a Fusione*. Bologna, Italy: Università di Bologna, 2022.

[30] M. Yazdani-Asrami et al., "Roadmap on artificial intelligence and Big Data techniques for superconductivity," *Supercond. Sci. Technol.*, vol. 36, no. 4, 2023, Art. no. 043501.

[31] M. Yazdani-Asrami et al., "Artificial intelligence methods for applied superconductivity: Material, design, manufacturing, testing, operation, and condition monitoring," *Supercond. Sci. Technol.*, vol. 35, no. 12, 2022, Art. no. 123001.

[32] A. Chipperfield and P. Fleming, *The MATLAB Genetic Algorithm Toolbox*. Natick, MA, USA: MATLAB, 1995.

[33] S. Ebbesen, P. Kiwitz, and L. Guzzella, "A generic particle swarm optimization matlab function," in *Proc. 2012 IEEE Amer. Control Conf.*, 2012, pp. 1519–1524.

[34] R. Mataira, M. Ainslie, A. Pantoja, R. Badcock, and C. Bumby, "Mechanism of the high-T_c superconducting dynamo: Models and experiment," *Phys. Rev. Appl.*, vol. 14, no. 2, 2020, Art. no. 024012.

[35] M. Ainslie et al., "A new benchmark problem for electromagnetic modelling of superconductors: The high-T_c superconducting dynamo," *Supercond. Sci. Technol.*, vol. 33, no. 10, 2020, Art. no. 105009.

[36] L. Fu, K. Matsuda, M. Baghdadi, and T. Coombs, "Linear flux pump device applied to high temperature superconducting (HTS) magnets," *IEEE Trans. Appl. Supercond.*, vol. 25, no. 3, Jun. 2015, Art. no. 4603804.

[37] M. Di Pietrantonio et al., "Design and performance of a linear flux pump for the frascati coil cold test facility," *IEEE Trans. Appl. Supercond.*, vol. 34, no. 3, May 2024, Art. no. 5700307.

[38] ENEA, "DTT - divertor tokamak test facility – interim design report," Apr. 2019. [Online]. Available: https://iris.polito.it/handle/11583/2736352

[39] P. Zito, M. Manganelli, A. Lampasi, S. Pipolo, and R. Lopes, "Final design of the DTT toroidal power supply circuit," *Fusion Eng. Des.*, vol. 192, 2023, Art. no. 113595.

[40] Y. Kim et al., "YBCO and Bi2223 coils for high field LTS/HTS NMR magnets: HTS-HTS joint resistivity," *IEEE Trans. Appl. Supercond.*, vol. 23, no. 3, Jun. 2013, Art. no. 6800704.

[41] J. H. Rice et al., "Design of a 60 kA flux pump for fusion toroidal field coils," *IEEE Trans. Appl. Supercond.*, vol. 32, no. 4, Jun. 2021, Art. no. 5500205.

[42] C. Hoffmann, R. Walsh, E. Karrer-Mueller, and D. Pooke, "Design parameters for an HTS flux pump," *Phys. Procedia*, vol. 36, pp. 1324–1329, 2012.

[43] W. Wang et al., "Test of two kilo-amp linear-motor type flux pumps with converged output current over 3.1 kA," *IEEE Trans. Appl. Supercond.*, vol. 34, no. 3, May 2024, Art. no. 5000305.

[44] M. Chiampi, C. Ragusa, and M. Repetto, "Fuzzy approach for multiobjective optimization in magnetics," *IEEE Trans. Magn.*, vol. 32, no. 3, pp. 1234–1237, May 1996.

[45] C. A. Borghi, M. Breschi, M. Fabbri, and I. Montanari, "Material optimization of ferromagnetic shields," *IEEE Trans. Magn.*, vol. 39, no. 3, pp. 1317–1320, May 2003.

Open Access funding provided by 'Alma Mater Studiorum - Università di Bologna' within the CRUI CARE Agreement